1

Rotor Aerodynamic Theory

1.1 Introduction

Theoretical background in energy extraction generalities and more specifically rotor aerodynamics of horizontal axis wind turbines (HAWTs) is developed in this chapter. Some prior knowledge of fluid dynamics in general and as applied to the analysis of wind turbine systems is assumed, in particular basic expressions for energy in a fluid flow, Bernoulli's equation, definitions of lift and drag, some appreciation of stall as an aerodynamic phenomenon and blade element momentum (BEM) theory in its conventional form as applied to HAWTs. Nevertheless some of this basic knowledge is also reviewed, more or less from first principles. The aim is to express particular insights that will assist the further discussion of issues in optimisation of rotor design and also aid evaluation of various types of innovative systems, for example those that exploit flow concentration.

Why focus much at all on theory in a book about innovative technology? Theory is often buried in more or less opaque computer code which may generate loads and information that engineers can use in design. However, as will be amplified in following chapters, theory is in itself;

- Food for innovation and suggestive of methods of performance enhancement or alternative concepts.
- A basis for understanding what is possible and providing an overview appraisal of innovative concepts.
- A source of analytic relationships that can guide early design at a stage where many key parameters remain to be determined and there are too many options to subject each to detailed evaluation.

Prior to discussions of actuator disc theory and the BEM theory that has underpinned most practical engineering calculations for rotor aerodynamic design and determination of wind turbine loads, some discussion of aerodynamic lift is presented. This is intended particularly to highlight a few specific insights which can guide design and evaluation of wind energy systems. In general, a much more detailed understanding of basic aerodynamics is required in wind turbine design. This must cover a wide range of topics, 2D and 3D flow effects in relation to aerofoil performance, stall behaviour, aeroelastic behaviour, unsteady

Innovation in Wind Turbine Design, First Edition. Peter Jamieson.

effects including stall hysteresis and induction lag, determination of suitable aerofoil data for wide ranges in angle of attack, and so on. References [1–10] are a sample from extensive published work covering some of these issues.

1.2 Aerodynamic Lift

The earliest wind turbines tended to use the more obvious drag forces [11] experienced by anyone exposed to wind on a windy day and use of the potentially more powerful lift forces was almost accidental. Exploitation of the aerodynamic lift force is at the heart of efficient modern wind turbines but surprisingly the explanation of lift has been quite contentious. Before entering that territory consider first Bernoulli's equation which is derived in many standard sources on fluid mechanics. Ignoring gravitational, thermal and other energy sources and considering only pressure, this equation becomes: $p + 1/2\rho V^2 = p_0$ where p is static pressure in a fluid element moving with a velocity of magnitude V, ρ is fluid density and p_0 is the total pressure which, in the absence of energy extraction, is constant along any streamline in the flow field.

Bernoulli's equation is essentially an energy equation which is expressed dimensionally in units of pressure and can be viewed as conservation of energy per unit volume of the fluid. In that connection, pressure can be regarded as the source potential energy (per unit volume) that drives fluid flow. This interpretation is discussed subsequently and is seen to be crucial to a clear understanding of how a wind turbine rotor works.

Returning to the issue of aerodynamic lift, one view of the explanation of the lift force has been that the fluid, should it have a longer path to traverse on one side of an aerofoil, will travel faster in order to meet the fluid flowing past the other side at the trailing edge of the aerofoil. With increase in velocity, the associated static pressure in that region will reduce in consequence of Bernoulli's equation. The pressure deficit on the side of the plate with the longer flow path is then considered the source of the lift force.

There are various problems with this as an explanation of the lift force. Firstly, a thin plate set at an angle in a uniform flow field will generate significant lift when, considering its shape, there is negligible difference between the upper surface and lower surface paths. Secondly, if an aerofoil with a shape with a noticeably longer flow path on one side is considered and the assumption that the flow on each side will traverse the length of the aerofoil in equal times (something in itself that can be challenged) is made, the difference in static pressure calculated on the basis of the implied velocities on each side of the aerofoil will be found quite insufficient to account for the observed lift force.

An apparently authenticated story relates to the efforts of the famous physicist Albert Einstein in aerofoil development. Einstein's effort, inspired by the path length related concept, was a miserable failure[1] and he later commented '*That is what can happen to a man who thinks a lot but reads little*.'

[1] According to Carl Seelig (*Albert Einstein: A Documentary Biography* by Carl Seelig, 1960, pp 251–252; Translated by Mervyn Savill, London: Staples Press, Bib ID 2263034), an accredited biographer of Einstein: 'It is not well known that... Einstein ...undertook a new aerofoil design intended for serial production. Eberhard, the chief test pilot, treated the fruit of the famous theoretician's efforts with suspicion.' 'Ehrhardt's letter continues (EA 59-556, as quoted in Folly 1955): A few weeks later, the "cat's back aerofoil" had been fitted to the normal fuselage of a LVG biplane, and I was confronted with the task of testing it in flight. ...I ... expressed the fear that the machine would react to the lack of angle of incidence in the wing by dropping its tail and would thus presumably be obliged to take off in an extremely unstable attitude. Unfortunately the sceptic in one proved to be right, for I hung in the air like a "pregnant duck" after take-off and could only rejoice when, after flying painfully

Considering the basic definition of lift as the force created on an object at right angles to the incident flow, it is evident that such a force, like all forces according to Newton's Second Law, will be associated with a rate of change of momentum in that direction. Thus the magnitude of the lift force will in principle be unambiguously determined by integrating all the components of momentum in the flow field normal to the incident flow that result from the object causing deviation of the flow.

Whilst this explanation is pure and fundamental it does not immediately shed light on why lift forces can be so large.

The explanation relating to Bernoulli's equation has some relevance here. Where flow is accelerated around a curved surface, the reduction in static pressure assists in maintaining attachment of the flow and contributes to large suction forces. As nature proverbially abhors a vacuum, strong suction on the boundary layer near a curved surface will induce a large deviation in the general fluid flow some distance from the surface thereby giving a large overall change in fluid momentum and producing a strong lift force. Aerofoil design is very much about the extent to which such forces can be sustained as the curvature is increased and more severe changes of flow direction are attempted in order to increase lift.

An associated consequence of the Bernoulli equation is the so-called Coanda effect. Aerofoils with elliptical section were developed and used on the X-wing plane/helicopter design [12]. Such aerofoils will have only moderate lifting capability attributable to their shape alone. However the discharge of a thin jet of air tangential to the surface near the trailing edge will attract the general flow to the jet and cause a much larger deviation in flow direction and consequently much enhanced lift.

The 'attraction' of the jet to the surface arises as the jet brings increased momentum into the boundary layer where the jet flow is next to the body surface. This overcomes the natural tendency of the (reduced momentum) boundary layer to separate under the adverse (rising) streamwise pressure gradient due to the aerofoil curvature. Due to the large curvatures involved, there is a noticeable pressure change across the jet which can be calculated from the mass flow rate in the jet and the radius of curvature of the flow. The jet tries to entrain any fluid between itself and the wall (very efficiently because it is normally turbulent) and this entrainment keeps it attached to the wall. Then, because the streamlines are now curved, the wall pressure falls below the external ambient value. In fact, in the absence of external flow incident on the aerofoil, such a jet will almost completely encircle the aerofoil.

This phenomenon is often called the Coanda effect in recognition of Henri-Marie Coanda who discovered it apparently through rather hazardous personal experience.[2] Controlling lift on an aerofoil section by blowing a jet tangential to the surface is often referred to as circulation control. It is a form of boundary layer control which has been considered for regulation of loads and control or performance enhancement of wind turbine blades [13].

Lift is intimately related to vorticity [14]. Associated with this is the Magnus effect, whereby a rotating cylinder (or sphere) can generate lift. This affects the flight of balls in many sports, has been employed in the form of the Flettner rotor [15] to power ships and has been exploited in at least two innovative wind turbine designs [16, 17]. Wikipedia [18]

down the airfield, I felt solid ground under my wheels again just short of the airfield at Aldershof. The second pilot had no greater success, not until the cat's back aerofoil was modified to give it an angle of incidence could we venture to fly a turn, but even now the pregnant duck had merely become a lame duck'.

[2] Henri Coanda was asked to devise a system to divert the hot jet discharges from an aircraft's engines away from the cockpit and fuselage. In blowing air to this end, the jet did exactly the opposite and attracted the hot gases to the fuselage surface with dangerous consequences.

is quite informative on lift, vorticity and the Magnus effect and also provides commentary on some popular incomplete views such as have been discussed.

Finally in the context of wind turbine systems, lift may also be involved in the performance of wind devices that have been casually categorised as 'drag' devices (see Section 13.2).

1.3 The Actuator Disc

The actuator disc is a valuable concept that arose early in the development of analyses of rotors and propellers. Without any specific knowledge of or assumptions about the system that may extract energy flowing through an arbitrary area in a uniform flow field, consideration of energy and momentum conservation allow some basic information about the consequent flow and limits on maximum possible energy extraction to be established.

This theory is summarised for a rotor (or other energy extraction device) in open flow (Figure 1.1). The analysis leads to Froude's theorem[3] and the well known Betz limit. In addition, actuator disc theory is further presented in a recently developed, more generalised form that will also deal with a rotor in *constrained* flow (Figure 1.2). Constrained flow is defined as the situation in which:

- an object is introduced into a flow field which modifies at least locally an otherwise uniform flow field of constant velocity;
- no energy is introduced or extracted by that object (conservative system).

An energy extraction device may then be introduced into the constrained flow field in principle anywhere but most usually in a region of *flow concentration* where there is a higher local velocity and hence higher mass flow though unit area normal to the flow than in the far upstream flow. Typical examples of constrained flow are where there is a hill, a duct or a diffuser.

In the context of evaluating innovation, the point of considering this more general situation is twofold. Understanding the limitations on power performance of wind farms in complex terrain (hills) is a mainstream concern. Although there are no mainstream large scale commercial wind energy systems that exploit flow concentration systems, nevertheless such systems have long been considered, some developed to prototype stage, and others are under present development. So they continue to receive increasing attention among innovative wind turbine designs.

Figure 1.1 represents a rotor in open flow. The flow field in the absence of the rotor would be of constant velocity everywhere and parallel to the axis of the rotor.

Figure 1.2 represents a rotor in a diffuser (toroid with aerofoil cross section as indicated). This is an example of constrained flow. Even in the absence of the rotor and of any energy extraction, the flow in a region around the diffuser is altered[4] by its presence and is substantially non-uniform.

[3] This is the result (for open flow) that the velocity at the rotor (energy extraction) plane is the average of the far upstream velocity and far wake velocity.

[4] It may also be noted that the ground itself, even if completely level, constrains the flow. Although the ground effect extends in all directions to infinity its constraint effect on the streamlines does exist locally near the wind turbine as if there is a mirror image of the turbine in the ground. It is not normally taken into account, but the effect is quite noticeable for example on the wake which because of its swirl lies at a small angle to the free stream. In contrast the wind shear effect associated with the ground boundary layer is not due to the normal velocity constraint and extends everywhere independent of the presence of the turbine.

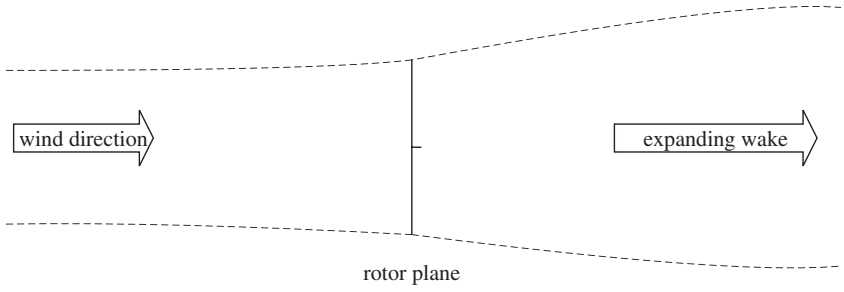

Figure 1.1 Open flow

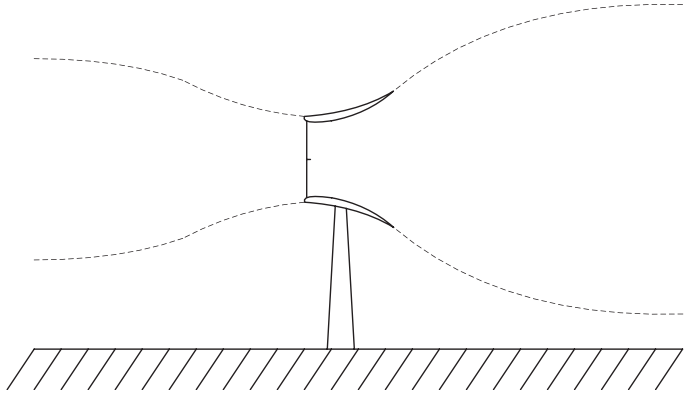

Figure 1.2 Constrained flow example (diffuser)

1.4 Open Flow Actuator Disc

1.4.1 Axial Induction

The axial induction at the rotor plane is defined as the fractional reduction in far upstream wind speed local to the rotor. Thus (see Figure 1.3) the velocity through the rotor plane is

$$V_1 = V_0(1 - a) \tag{1.1}$$

Considering change in kinetic energy between far upstream and far wake, the power (rate of change of kinetic energy) extracted P is:

$$P = \frac{1}{2}\rho A_0 V_0^3 - \frac{1}{2}\rho A_2 V_2^3 \tag{1.2}$$

From continuity of flow, $\rho A_0 V_0 = \rho A_2 V_2$. Hence:

$$P = \frac{1}{2}\rho A_0 V_0 \left(V_0^2 - V_2^2\right) \tag{1.3}$$

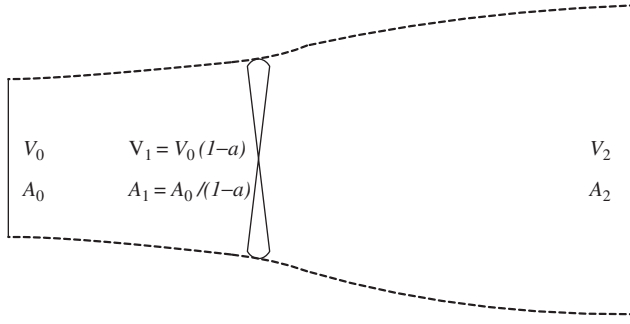

Figure 1.3 Open flow actuator disc model

1.4.2 Momentum

The mass flow rate through rotor plane is $\rho A_1 V_1$. The change in fluid velocity between upstream far wake is $(V_0 - V_2)$. Hence, rotor thrust as rate of change of momentum through the rotor plane is

$$T = \rho A_1 V_1 (V_0 - V_2) \tag{1.4}$$

and power, P is

$$P = T V_1 \tag{1.5}$$

$$= \rho A_0 V_0^2 (1 - \mathrm{a}) (V_0 - V_2) \tag{1.6}$$

From Equations 1.3 and 1.6:

$$V_2 = V_0 (1 - 2a) \tag{1.7}$$

Thus the far wake induction is twice the value at the rotor plane. This result was first derived by Froude [19]. Defining power coefficient C_p as the ratio of fraction of energy extracted by the rotor to the amount that would pass through the rotor swept area with the rotor absent, then:

$$P = \frac{1}{2} \rho A V^3 C_p \tag{1.8}$$

Considering Equation 1.8 and substituting for V_2 from equation in Equation 1.3 leads to

$$C_p = 4a (1 - a)^2 \tag{1.9}$$

Differentiating Equation 1.9 to determine a maximum leads to $a = 1/3$ and to the Betz limit:

$$C_p = 16/27 \tag{1.10}$$

Investigations by Bergey [20] and van Kuik [21] indicated that Lanchester (1915), Betz (1920) and Joukowski (1920) may all have, probably independently and certainly by methods differing in detail, determined the maximum efficiency of an energy extraction device in open flow. Most recently, further investigation by Okulov and van Kuik [22] suggests that the attribution to Lanchester by Bergey is inappropriate. Thus the Betz limit

may perhaps most properly be called the Betz-Joukowski limit although for convenience the short reference as Betz limit is retained.

Although open flow actuator disc theory is some 90 years old, it is by no means 'done and dusted'. Van Kuik [23] in considering edge effects at the disc suggests that the axial induction at the rotor may be less than predicted by the foregoing simple model and hence the velocity at the rotor plane greater than $\frac{V_0+V_2}{2}$. Others consider a similar outcome to be due to external flows assisting transport of the wake and therefore contributing additional energy to the system. It should be noted that the actuator disc models in their basic form deal only with inviscid flow.

1.5 Generalised Actuator Disc Theory

Especially among innovative wind turbine systems, there has been continuing interest in concepts to augment or concentrate flow with the idea that a smaller, lighter, perhaps faster and certainly less expensive rotor can extract as much energy as a large rotor in open flow. Of course these benefits must be traded against the cost of the system that augments the flow. The usual means of augmentation is by placing the rotor in a duct or diffuser which serves to induce extra mass flow through the rotor as compared to open flow. More exotic concepts have also been considered using vanes [24] or a delta wing [25] to induce vortices creating regions of intensified flow. Coming down to earth, quite literally, the least exotic and most commonplace flow augmenter is a hill top.

In spite of the longstanding interest in flow concentration systems, in ducted rotors and the longevity of the Betz result (Equation 1.10) for wind turbines in open flow, until recently there was no corresponding theory to specify the ideal limiting performance of wind turbines in ducts or diffusers, or more generally in non-uniform flow fields, although Betz was aware that his limit could be exceeded. The power coefficient, C_p, is defined in terms of the area of the energy extraction device and the Betz limit can be exceeded if additional mass flow is induced through the area of the device, say by a duct or diffuser.

In the early 1980s, Oman, Gilbert and Foreman [26] conducted experimental work on the diffuser augmented wind turbine (DAWT) concept showing that power coefficients exceeding the Betz limit could be obtained. In 1999, Hansen [27] published computational fluid dynamics (CFD) results confirming that the Betz limit could be exceeded. Hansen noted that the increase in C_p was in proportion to the augmentation of mass flow achieved by the diffuser but that this did not explicitly define a limit for C_p.

Although the open flow actuator disc theory which determines the Betz limit has evidently been established for over 90 years and van Bussel [28] in a comprehensive review notes that diffuser research has been in progress over 50 years, the generalisation of actuator disc theory arises from recent analysis by Jamieson [29]. This work includes new relationships for limiting values of C_p and a preliminary validation has shown close quantitative agreement with Hansen's CFD results [27].

In many previous analyses of turbines in ducts and diffusers, speed up factors are introduced and definitions of C_p and C_t other than the standard ones have been employed. This is understandable in the historical context but there is no longer need for it and some potential for confusion. The following analysis maintains standard definitions of axial induction, power and thrust coefficients.

Axial induction, a, at the rotor plane is defined exactly as before (Equation 1.1). Thus if the flow is augmented at the rotor plane, a is negative.

As in open flow, the power coefficient and thrust coefficient are defined with respect to the far upstream wind speed and referenced to the rotor swept area. They are respectively

$$C_p = \frac{P}{\frac{1}{2}\rho A V_0^3} \tag{1.11}$$

and

$$C_t = \frac{T}{\frac{1}{2}\rho A V_0^2} \tag{1.12}$$

From these basic definitions of the power co-efficient, C_p, and the thrust co-efficient, C_t, the power to thrust ratio can be expressed as in Equation 1.13:

$$\frac{P}{T} = V_0.\frac{C_p}{C_t} \tag{1.13}$$

However considering also the basic definition of power as a product of force and velocity as applied at the rotor plane:

$$P = T V_0 (1 - a) \tag{1.14}$$

Hence

$$\frac{P}{T} = V_0 (1 - a) \tag{1.15}$$

Hence, from Equations 1.13 and 1.15,

$$\frac{C_p}{C_t} = (1 - a) \tag{1.16}$$

Equation 1.16 is completely general for any system with a rotor where the local inflow is a fraction $(1 - a)$ of the remote undisturbed external wind speed.

A system is defined as the region in which axial induction is influenced between the freestream and the far wake. Energy extraction is considered to take place across a planar area normal to the flow and at a definite location within the system.

Let $f(a)$ be the axial induction in the far wake (Figure 1.4). At any plane of area A within the system where there is a pressure difference, Δp associated with energy extraction, the thrust, T is given as:

$$T = \Delta p A = \frac{1}{2}\rho V_0^2 A C_t \tag{1.17}$$

Hence

$$C_t = \frac{2\Delta p}{\rho V_0^2} \tag{1.18}$$

Considering Bernoulli's equation applied upwind of the extraction plane:

$$p_0 + \frac{1}{2}\rho V_0^2 = p_1 + \frac{1}{2}\rho V_0^2 (1 - a)^2 \tag{1.19}$$

and on the downstream side of the extraction plane

$$p_1 - \Delta p + \frac{1}{2}\rho V_0^2(1-a)^2 = p_0 + \frac{1}{2}\rho V_0^2\{1 - f(a)\}^2 \tag{1.20}$$

From Equations 1.18–1.20:

$$C_t = 1 - \{1 - f(a)\}^2 \tag{1.21}$$

that is

$$C_t = 2f(a) - f(a)^2 \tag{1.22}$$

Now consider that:

1. For energy extraction to take place the velocity in the far wake must be less than ambient, that is $f(a) > 0$
2. If the flow is augmented above ambient at the rotor plane, then purely from considerations of continuity, there must exist a reference plane of area A_{ref} downstream of the rotor plane where the induction is half that of the far wake, that is $= \frac{f(a)}{2}$.

Considering conservation of mass in the flow, then:

$$\rho A V_0 (1-a) = \rho A_{\text{ref}} V_0 \left(1 - \frac{f(a)}{2}\right) \tag{1.23}$$

In the absence of energy extraction, note that $f(a) = 0$ and let the axial induction at the energy extraction plane be a_0:

$$\rho A V_0 (1 - a_0) = \rho A_{\text{ref}} V_0 \tag{1.24}$$

Hence from Equations 1.23 and 1.24

$$f(a) = 2\left\{\frac{a - a_0}{1 - a_0}\right\} \tag{1.25}$$

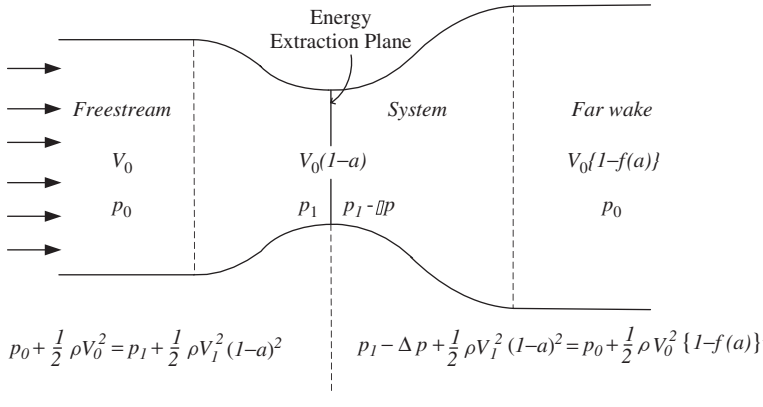

Figure 1.4 General flow diagram

Now substituting for $f(a)$ in Equation 1.22 gives:

$$C_t = \frac{4(a - a_0)(1 - a)}{(1 - a_0)^2} \tag{1.26}$$

And hence from Equation 1.16

$$C_p = \frac{4(a - a_0)(1 - a)^2}{(1 - a_0)^2} \tag{1.27}$$

Differentiating Equation 1.27 with respect to a determines a maximum at $a = a_{\mathrm{m}}$ of

$$a_{\mathrm{m}} = \frac{1 + 2a_0}{3} \tag{1.28}$$

The associated maximum C_p is then:

$$C_{\mathrm{pm}} = \frac{16}{27}(1 - a_0) \tag{1.29}$$

For the open flow rotor with $a_0 = 0$, Equations 1.26–1.29 correspond, as they must, to the established equations for open flow. The familiar results that the open flow rotor operates optimally when $a_{\mathrm{m}} = 1/3$ and has an associated maximum power coefficient $C_{\mathrm{pm}} = 16/27$ (the Betz limit) are evident.

A more striking result falls out of the limit Equation 1.26. On substituting for a_{m} from Equation 1.28 in Equation 1.26, it is found that

$$C_t = 8/9 \tag{1.30}$$

Whereas a_{m} and C_{pm} have specific values for each system configuration, this result is now independent of a_0. Equation 1.30 is therefore a general truth for an optimum energy extraction device in any ideal system configuration.

This result was mentioned to the author in 1995 by K. Foreman, as an observed outcome (without theoretical explanation) of his extensive experimental work within Grumman Aerospace in the 1980s with the DAWT concept. It was proven more recently by van Bussel [28] and now directly as a consequence of the generalised limit: Equations 1.26 and 1.28.

Considering Equation 1.18, a corollary to Equation 1.30 is that the pressure drop across the rotor plane for optimum energy extraction is always $4/9\rho\ V_0^2$.

Thus in any flow field of uniform far upstream velocity, V_0, *regardless of what local flow augmentations are created (conservatively) within the system and wherever a rotor is located*, the rotor will, in optimum operation to maximise power extraction, experience the same loading in terms of thrust, T, thrust coefficient C_t and rotor plane pressure drop Δp. This does not in the least contradict statements in many sources (e.g. Lawn [30]) that a rotor in augmented flow must be 'lightly loaded'. Loading it at the same level of thrust as would be optimum in open flow, when the wind speed local to the rotor may be several times greater than ambient, amounts to very 'light' loading. The level of loading is independent of the level of flow augmentation achieved by the diffuser and will therefore appear all the lighter, the greater the flow augmentation.

Results are summarised in Table 1.1.

Table 1.1 Summary results comparing open and constrained flow

General operation		
	Betz open flow	Generalised constrained flow
Upstream wind speed	V_0	V_0
Wind speed at energy extraction plane	$V_0\,(1-a)$	$V_0\,(1-a)$
Far wake wind speed	$V_0\,(1-2a)$	$V_0\left(\dfrac{1-2a+a_0}{1-a_0}\right)$
Performance coefficient, C_p	$4a\,(1-a)^2$	$\dfrac{4\,(a-a_0)\,(1-a)^2}{(1-a_0)^2}$
Thrust coefficient, C_T	$4a\,(1-a)$	$\dfrac{4\,(a-a_0)\,(1-a)}{(1-a_0)^2}$
Pressure difference across rotor	$\dfrac{1}{2}\rho V_0^2 C_T$	$\dfrac{1}{2}\rho V_0^2 C_T$
Optimum performance		
	Betz open flow	Generalised constrained flow
Maximum, C_p	$\dfrac{16}{27}$	$\dfrac{16}{27}\,(1-a_0)$
Associated axial induction factor	$\dfrac{1}{3}$	$\dfrac{1+2a_0}{3}$
Far wake axial induction factor	$\dfrac{2}{3}$	$\dfrac{2}{3}$
Associated thrust coefficient	$\dfrac{8}{9}$	$\dfrac{8}{9}$
Pressure difference across rotor	$\dfrac{4}{9}\rho V_0^2$	$\dfrac{4}{9}\rho V_0^2$

Consider now Figure 1.5 where instead of fixing the rotor swept area, the source flow area is fixed. With the same source flow area, the source mass flow rate and source power is the same in all three cases, namely, the general case with an arbitrary system, the particular case of a diffuser concentrator and the standard case in open flow.

From Equation 1.29:

$$C_\mathrm{pm} = \frac{16}{27}\,(1-a_0)$$

Energy extracted by the rotor is by definition:

$$E_1 = \frac{1}{2}\rho V_0^3 A_1 C_\mathrm{pm}$$

From continuity of flow:

$$E_1 = \frac{1}{2}\rho V_0^3 \frac{A_0}{(1-a_\mathrm{m})} C_\mathrm{pm}$$

Using Equations 1.28 and 1.29

$$E_1 = \frac{1}{2}\rho V_0^3 A_0 \frac{8}{9}$$

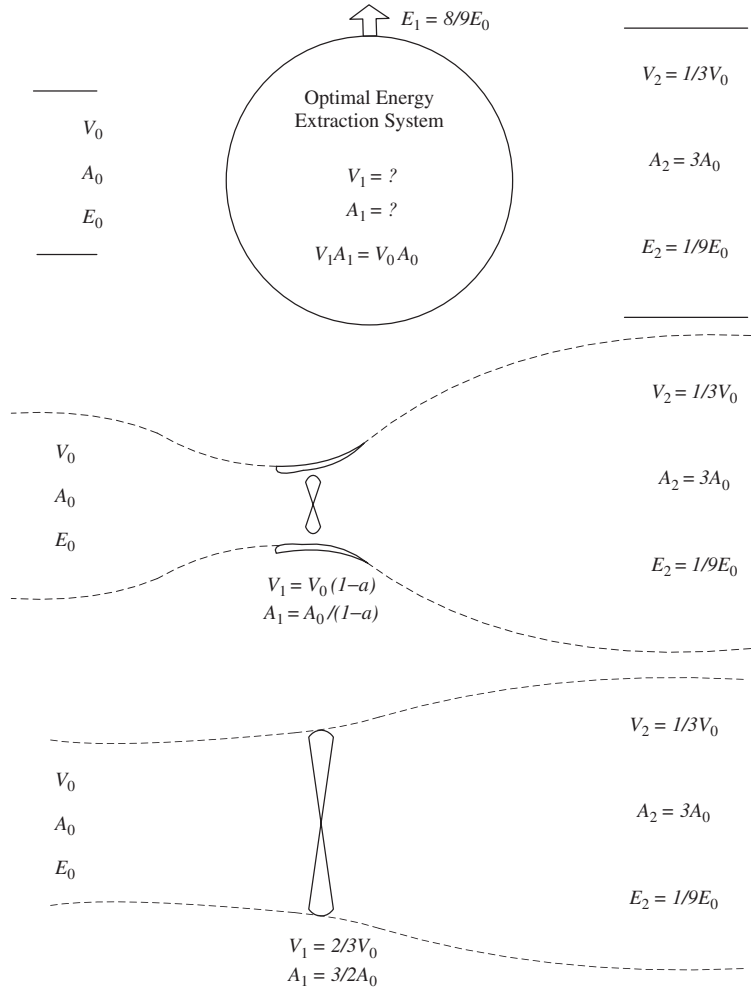

Figure 1.5 Comparison of cases with equal source flow areas

This evidently is 8/9 of the kinetic energy in the upstream source area. Thus the equation system (Equations 1.27–1.31) confirms a plausible result:

> Regardless of whether the flow is open or constrained (say by a hill or diffuser), 8/9 of source upstream kinetic energy is the maximum fraction extractable from an energy extraction device located anywhere in its associated streamtube.
>
> Moreover the optimum specific loading on the energy extraction device is always the same and corresponds to, $C_t = 8/9$.

In the open flow case, the 'system' is always 'ideal' in that the flow is unconstrained and free to flow through or around the rotor in a way that can vary with rotor loading. In all other cases, the system comprises some physical entity additional to the rotor which constrains the

flow. In general this system, whether hill, diffuser or other, because it is of fixed geometry, will not be ideal in every flow state and may not be ideal in any. Hence even in terms of purely inviscid flow modelling, such systems, regardless of the efficiency of the rotor or energy extraction device, may not extract energy as efficiently as in open flow. Comparing an effective diffuser system with an open flow rotor that optimally extracts the same amount of energy, the rotor in the diffuser system can be much smaller in diameter and the critical design issue is whether this advantage can justify the cost of the diffuser system.

In the limit state (ideal device in ideal system):

- The design of the device is completely decoupled from design of the system which system is completely characterised by a_0.
- The thrust and thrust coefficient that corresponds to optimum rotor loading are independent of the system that includes the rotor and the thrust coefficient is always 8/9.

The conclusion from this is that for any system influencing the local flow through an energy extraction device, the induction factor, a_0, at the extraction plane with the device absent provides a characteristic signature of the system. This statement is probably valid for non-ideal energy extraction devices such as rotors with drag loss, tip loss and swirl loss providing the system influencing the rotor plane induction is ideal.

1.6 The Force on a Diffuser

From Equation 1.24, the mass flow rate through the energy extraction plane (and elsewhere) is, $\rho A V_0 (1-a)$ and from Equation 1.25, the change in fluid velocity between far upstream and far downstream is, $f(a) = 2\left\{\frac{a-a_0}{1-a_0}\right\}$. Hence the rate of change of momentum and total thrust force on the system is the product of these quantities.

$$T_{net} = (\rho A V_1)\left\{\frac{2V_0(a-a_0)}{(1-a_0)}\right\} = \frac{1}{2}\rho A V_0^2\left\{\frac{4(1-a)(a-a_0)}{(1-a_0)}\right\} \tag{1.31}$$

Now thrust on the rotor is by definition:

$$T = \frac{1}{2}\rho A V_0^2 C_T$$

And hence from Equation 1.26:

$$T = \frac{1}{2}\rho A V_0^2\left\{\frac{4(1-a)(a-a_0)}{(1-a_0)^2}\right\} \tag{1.32}$$

Comparing Equations 1.31 and 1.32 it is clear that the force on the diffuser is

$$T_d = \frac{1}{2}\rho A V_0^2\left\{\frac{-4a_0(1-a)(a-a_0)}{(1-a_0)^2}\right\} = -a_0 T \tag{1.33}$$

This very simple result is important. The separation of total system thrust into the part that acts on the rotor or energy extraction device and the part that acts on the diffuser or flow concentrator is vital for an appropriate implementation of BEM theory to deal with modelling of system loads or optimisation of rotors in constrained flows. Note also that, as far as inviscid flow is concerned, although thrust on the diffuser may be several times that

on the rotor, thrust on the diffuser only appears in association with rotor loading and is zero on the empty duct. The simple form of Equation 1.33 provides insight but applies only to an ideal diffuser.

Considering the diffuser as an axisymmetric aerofoil body, suction on the leading edge may in general produce a thrust component that is directed into wind. The net force on the diffuser is then the sum of suction forces and pressure drag forces. When the diffuser is not ideal, the ratio of net force on diffuser to force on the rotor is increased and exceeds the prediction of Equation 1.33.

1.7 Generalised Actuator Disc Theory and Realistic Diffuser Design

The analysis presented here of ducts or diffusers in inviscid flow is only the starting point. The generalised actuator disc theory:

1. is a limiting theory only (as is the Betz theory in open flow) that considers only inviscid flow;
2. shows clearly why flow concentration devices increase available energy at best linearly as increase of mass flow and not as the cube of the augmented velocity;
3. describes ideal systems whereas real diffusers may be far from the limiting performance suggested. In general their fixed geometry will only best suit one state of loading. The Kutta condition associated with the finite thickness of the aerofoil duct sections will in general (even at the level of potential flow) lead to reduced performance of diffusers;
4. as an inviscid model, does not capture effects of flows external to the diffuser and rotor which can be used to augment performance through viscous interactions. Some diffusers are very much designed to exploit such effects as in the FloDesign wind turbine [31].

These comments serve to underline that while generalised actuator disc theory affords some valuable new insights and provides energy limits for ideal systems, there is quite a gap between such ideal limiting theory and real world design of flow augmenters.

1.8 Why a Rotor?

The actuator disc idea considers an arbitrary energy extraction system which need not be a rotor. Yet all present mainstream wind energy conversion systems rely on the rotor concept. Why? A wind energy system is not only, as is axiomatic, an energy conversion system turning fluid mechanical energy in the wind into electrical energy, but is also an energy concentration system.

For example a typical modern 1.5 MW wind turbine may have parameters as in Table 1.2. In a case when the wind turbine is producing its rated output (1500 kW in the electrical cables), it has received wind energy over the swept area at a power density $\sim$1 kW/m^2 and is transporting output after losses at a power density of over 1 GW/m^2. As the power passes through the system, it is concentrated first in the composite of the blades, then in the steel of the shaft, subsequently in the field of the generator and finally in the copper of the electrical cables.

It is vital to effect this massive concentration with as little cost as possible and the first major gain is made in the rotor itself. The rotor typically has a solidity $\sim$5% and hence less

Table 1.2 Power concentrations in a 1.5 MW wind turbine

	D (m)	Area (m^2)	Efficiency	Power (kW)	Power density (kW/m^2)	Concentration factor	Cumulative concentration factor
Wind over swept area	70.5	3903.6	1.00	3636	0.932	1.0	1
Rotor blades input	70.5	204.0	0.44	3636	18	**19.1**	19
Low speed shaft input	0.564	0.2498	1.00	1611	6 449	361.7	6 923
Gearbox input	0.564	0.2498	0.98	1611	6 449	1.0	6 923
Generator input	0.120	0.0113	0.95	1579	139 610	21.6	149 870
Electrical cables	–	0.0010	1.00	1500	1 500 000	10.7	1 610 244

blade frontal area than the swept area by a factor ~20. This is evident in the highlighted concentration factor (**19.1**, in Table 1.2).

This is the key factor in favour of the rotor concept. The rotor can confront all the extractable energy in the swept area with blades that may occupy only about 5% of the swept area. This is in direct contrast to a translating aerofoil or say an oscillatory wave energy device where, although the source energy density is usually much greater than for wind, a metre length of wave energy converter must confront each metre of wave front from which energy is to be extracted.

Thus an efficient rotor is typically concentrating the extractable energy in the rotor disc by a factor of about 20 and so reducing the size and cost of the primary collectors (blades) compared with alternative systems such as an oscillating aerofoil that do not have this benefit. The answer to 'why a rotor?' is therefore not only the legitimate common observation that mechanical energy in rotational form best suits conventional electricity generating systems but also that, in sweeping an area of the source energy flux that is much greater than the physical surface area of the rotor blades, the rotor effects a significant primary increase in energy density.

This is the main reason why the rotor concept is very hard to beat and why many of the alternatives such as oscillating or translating aerofoils that are perfectly feasible technically may struggle to be cost competitive.

1.9 Basic Operation of a Rotor

The actuator disc model requires continuity of the fluid axial velocity through the rotor plane. This is essential as the wind turbine removes energy from the air flow passing through it but does not remove any of the air itself! Hence there is no change in axial velocity on either side of the disc and hence *no kinetic energy is extracted from the fluid at the rotor plane*. Yet a wind turbine rotor is generally described as a device for extracting kinetic energy from natural wind flow. In a global sense this is true; locally at the rotor plane it is not. Considering the overall energy balance between far upstream and far downstream in

the ideal inviscid model (as in Equation 1.2), kinetic energy has been extracted from the flow. This is because of the assumption that in the far wake the flow that passed through the rotor has returned to atmospheric static pressure. The energy change associated with the reduced axial velocity in the far wake is then seen as a net change in kinetic energy.

If locally the wind turbine rotor is not extracting kinetic energy and yet the system is producing power and therefore extracting energy from the fluid, what is the energy source? The answer is *potential energy*. A wind turbine rotor produces power from the torque generated by the rotor blades. This torque arises from forces on blade elements which in turn are the consequence of pressure differences on each side of the aerofoils. The wind turbine works by offering an appropriate resistance to the fluid flow slowing the fluid approaching the rotor. The reduction in fluid velocity occurs conservatively ahead of the rotor plane. Hence considering Bernoulli's equation, a rise in static pressure occurs to provide conservation of energy per unit volume. The pressure difference across the rotor plane in conjunction with the through flow velocity is then the determinant of the energy extraction and, as was discussed previously, pressure is effectively potential energy per unit volume of fluid.

Thus the basic equation for power at the rotor plane is:

$$P = \Delta p A_1 V_1 \tag{1.34}$$

This defines power extracted from the air flow and is an upper bound which is reduced by inefficiencies in the rotor and drive train. Consider now the operation of a rotor in constrained flow. The internet is littered with web sites where claims are made to the effect that some innovative system around a wind turbine increases the air velocity locally by a factor k and therefore the power as k^3.

In any area of flow augmentation prior to energy extraction, the flow concentrator does not introduce extra energy into the flow field. Therefore increased local velocity and the associated increased in local kinetic energy is created conservatively. Hence, according to Bernoulli's theorem, increased kinetic energy is obtained at the expense of static pressure (atmospheric potential energy). It is perfectly true that the kinetic energy locally is increased by a factor k^3. This must be the case by definition. However, as has been strongly emphasised, there is no extraction of kinetic energy at the rotor plane. It is the pressure difference at the rotor plane that drives energy extraction and both the inlet and exit pressure of an energy extraction device in a region of concentrated flow are at sub-atmospheric pressure. This means that much less energy can be extracted than might be supposed.

Perhaps the simplest way to appreciate this is as follows. Consider a fixed area, A_0, represented by the dotted lines of Figure 1.6, where a rotor may be placed but for the present in the absence of energy extraction. If the velocity is increased over the prevailing upstream value, V_0, by a factor say 3 in a flow augmentation device, the streamtube passing through it, by conservation of mass flow, will have an upstream source area that is 3 times greater than the extraction area, A_0. It then clear that no more than 3 times the energy and certainly not 3^3 times can be extracted from this streamtube.

In Equation 1.34, $V_1 = V_0(1 - a)$ as defined in Equation 1.1. If the rotor is in a concentrator, a will be negative of a magnitude related to the flow augmentation factor, k (which it should be noted will change with rotor loading). Noting the results of Table 1.1, it can be seen that, for maximum energy extraction, in open flow or constrained flow, Equation 1.34 is unchanged. Hence the increase in power is only linearly as the increase in local velocity in the region of flow concentration.

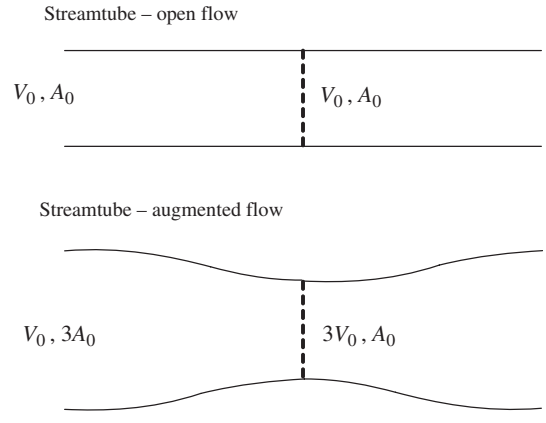

Figure 1.6 Source area and energy gain with flow augmentation

The generalised actuator disc theory implies that all rotors whether large or small, whether in open flow or in well optimised diffusers or other concentrators will operate optimally in an optimal system with a similar pressure difference across the rotor plane. This pressure difference under such ideal circumstances is $4/9\rho V_0^2$ (see Table 1.1). However in constrained flow fields, system inefficiencies (which importantly can arise from purely geometric aspects in addition to frictional losses) will in general further reduce the optimal pressure difference for maximum energy extraction.

1.10 Blade Element Momentum Theory

BEM theory is the most widely used theory in practical design methods and computer codes for predicting loads and performance of wind turbines. In any balanced overview of wind turbine modelling techniques reflecting current research directions, much attention would be devoted to vortex theories and CFD. These and numerical methods in general are not discussed. They may offer more accurate analysis of specific configurations but they do not yield analytical relationships that can provide physical insight to guide parametric evaluations and concept design.

In BEM, the swept area of the rotor is considered as a set of annular areas (Figure 1.7) swept by each blade element. The blade is divided spanwise into a set of elements which are assumed to be independent of each other so that balance of rate of change of fluid momentum with blade element forces can be separately established for each annular area. The basic theory is due to Glauert [32] with the modern forms for numerical implementation in BEM codes having developed following the adaptation of Glauert's theory by Wilson, Lissaman and Walker [33]. BEM theory is summarised here in order to preserve a self contained account of some new equations that are developed from it.

1.10.1 Momentum Equations

Considering thrust as rate of change of linear momentum of the flow passing through an annulus at radius r of width dr and denoting a tip effect factor (to be discussed) as F;

$$\text{Thrust} \quad dT = 4\pi\rho r V^2 a(1-a)F dr \tag{1.35}$$

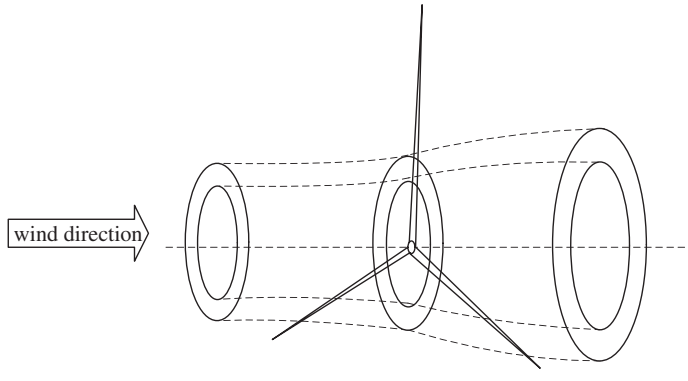

Figure 1.7 Actuator annulus

and similarly considering torque and rate of change of angular momentum:

$$\text{Torque} \quad dQ = 4\pi\rho r^3 V a'\omega(1-a)Fdr \tag{1.36}$$

1.10.2 Blade Element Equations

Considering blade element forces on a blade elements at radius r of width dr;

$$\text{Thrust} \quad dT = \frac{1}{2}\rho W^2 Bc(C_l\cos\varphi + C_D\sin\varphi)dr \tag{1.37}$$

$$\text{Torque} \quad dQ = \frac{1}{2}\rho W^2 Bc(C_L\sin\varphi - C_D\cos\varphi)rdr \tag{1.38}$$

Equations 1.35–1.38 allow dT and dQ to be eliminated yielding two equations in the three unknowns, a, a' and φ. A third equation is given by considering the flow geometry local to each blade element at radius, r, that is at radius fraction, $x = r/R$.

From the flow geometry (Figure 1.8):

$$\tan\varphi = \frac{V(1-a)}{\omega r(1+a')} = \frac{(1-a)}{\lambda x(1+a')} \tag{1.39}$$

Equating Equation 1.35 with Equation 1.37 and Equation 1.36 with Equation 1.38 to solve for the induced velocities a and a' (also making use of Equation 1.39) gives

$$\frac{a}{1-a} = \frac{\sigma(C_L + C_D\tan\varphi)}{4F\tan\varphi\sin\varphi} \tag{1.40}$$

$$\frac{a'}{1+a'} = \frac{\sigma(C_L\tan\varphi - C_D)}{4F\sin\varphi} \tag{1.41}$$

where σ, the local solidity, is defined as $\sigma = \frac{Bc}{2\pi r}$.

Usually an iterative procedure is used to solve Equations 1.39–1.41 for each local blade element of width Δr. Hence using Equations 1.37 and 1.38 the thrust and torque can be found on the whole rotor by integration.

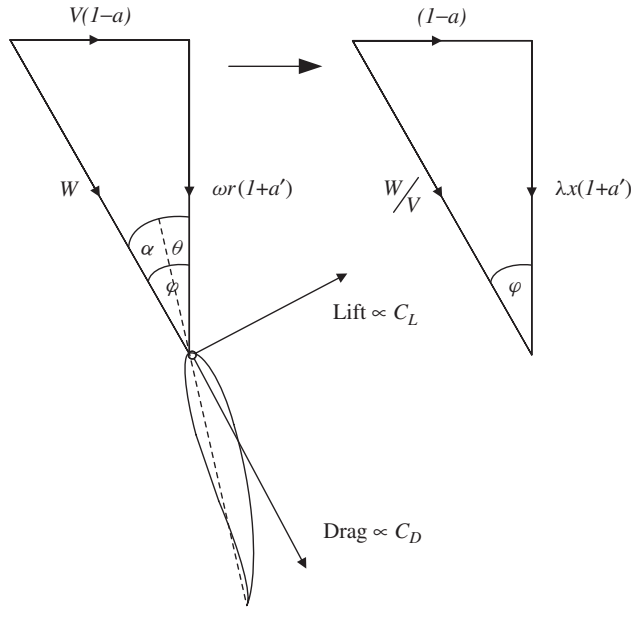

Figure 1.8 Local flow geometry at a blade element

The BEM analysis of Equations 1.35–1.38 has followed the widely used formulation of Wilson, Lissaman and Walker [33], who suggested that drag should be neglected in determining the induction factors, a and a'. According to the PhD thesis of Walker [34]:

> ... it has been the assumption that the drag terms should be omitted in calculations of a and a' ... on the basis that the retarded air due to drag is confined to thin helical sheets in the wake and (will) have negligible effect on these factors.

Although drag must be accounted in determining the torque and power developed by a rotor, opinion is divided[5] about whether the drag terms should be included in evaluation of the induction factors. Neglecting drag will generally lead to simpler Equations 1.40 and 1.41 and also simplify the following analyses.

From Equation 1.40,

$$\frac{a}{1-a} = \left(\frac{Bc}{2\pi r}\right)\frac{C_L\cos\varphi + C_D\sin\varphi}{4F\sin^2\varphi} \tag{1.42}$$

$$= \frac{B}{8\pi}\left(\frac{cC_L}{R}\right)\left(\frac{R}{r}\right)\frac{(\cos\varphi + C_D/C_L\ \sin\varphi)}{F\sin^2\varphi} \tag{1.43}$$

The term (cC_L/R) represents a non-dimensional lift distribution where the chord distribution $c \equiv c(\lambda, x)$ is in general a function of radius fraction, $x = r/R$, and design tip speed ratio, λ.

[5] GL Garrad Hassan use the formulation including drag as presented in Equations 1.40 and 1.41 in their commercial BEM code, Bladed.

Let $\Lambda(\lambda, x) = \frac{c(\lambda,x)C_L}{R}$, and let $k = \frac{C_L}{C_D}$:
Then

$$\frac{a}{1-a} = \frac{\Lambda B}{8\pi x F} \frac{\left[1 + (1/k) \quad \tan\varphi\right]}{\sin\varphi \quad \tan\varphi} \tag{1.44}$$

and

$$\sin\varphi = \frac{(1-a)}{\sqrt{(1-a)^2 + \lambda^2\, x^2(1+a')^2}} \tag{1.45}$$

Hence, after some manipulation:

$$\Lambda(\lambda, x) = \frac{8\pi a(1-a)}{B\lambda\,(1+a')\ \sqrt{(1-a)^2 + \lambda^2\, x^2(1+a')^2}} \quad \frac{F}{\left[1 + \frac{(1-a)}{k\,\lambda\, x(1+a')}\right]} \tag{1.46}$$

The tangential induction factor, a', can be solved as in Equation 1.47 in terms of a using Equations 1.39–1.41 to eliminate φ.

$$a' = \frac{\left\{\lambda^2 k^2 x^2 + 2\lambda k x - 4ak\left[\lambda x - k\,(1-a)\right] + 1\right\}^{0.5} - (\lambda k x + 1)}{2\,\lambda\, k\ x} \tag{1.47}$$

Note that the elimination of φ in Equations 1.46 and 1.47 is only apparent as the lift to drag ratio, k, depends in general on the angle of attack, α, and $\alpha = \varphi\,(x) - \theta\,(x) - \psi$ where $\theta\,(x)$is the blade twist distribution and ψ is the pitch angle of the blade.

In the limit of zero drag when $k \to \infty$:

$$a' = \frac{\left(4a - 4a^2 + \lambda^2 x^2\right)^{0.5} - \lambda x}{2\lambda x} \tag{1.48}$$

Equation 1.48 also appears in Manwell [35].

With further approximation:

$$a' = \frac{a\,(1-a)}{\lambda^2 x^2} \tag{1.49}$$

1.11 Optimum Rotor Theory

Optimum states are simpler to describe than general conditions. An analogy is that only three coordinates will define the summit of a hill whilst infinitely many may be required to characterise the whole surface.

In the optimum state, for typical rotors designed for electricity production with design tip speed ratios above 6, the tangential induction factor, a', should be small over the significant parts of span ($x > 0.2$). It may be neglected with little loss of accuracy in $\Lambda(\lambda, x)$ or calculated from Equations 1.47, 1.48 or 1.49.

The actuator disc result of Betz [36] establishes an optimum rotor thrust loading corresponding to a value of the thrust coefficient, $C_t = 8/9$. This implies an optimum lift force on each blade element which in effect specifies the product, cC_L, in Equation 1.37. Referring to Equation 1.38, it is plausible that with cC_L fixed, performance is maximised if C_D is minimum and hence k is maximum. Thus in the optimum operational state of a wind

turbine rotor, each blade element operates at maximum lift to drag ratio and the only aerofoil data required to define this state therefore is the maximum lift to drag ratio, k and the lift coefficient, C_L, associated with this maximum lift to drag ratio for each element over the span of a blade. Optimum performance at maximum lift to drag ratio is not exactly true (see later discussion around Equation 1.63) but is a satisfactory approximation for mainstream designs with design tip speed ratio above 6.

For a lift to drag ratio, $k = 100$, design tip speed ratio, $\lambda = 9$ and considering an optimum rotor with $a = 0.3333..$ at mid span where $x = 0.5$, Equations 1.47 and 1.48 give values for a' of 0.01010 and 0.01097 a difference in the optimum rotor state of around 10% albeit in a rather small quantity compared to the axial induction, a.

The square bracketed term in the denominator of Equation 1.46 which contains the lift to drag ratio k is effectively unity over the significant region of span for typical modern large rotors with design tip speed ratio > 6 and $k \geq 100$.

The lift produced by an aerofoil section can be associated with a bound circulation which is virtual over the span of the blade but becomes a real vortex at the end of blade where there is no material to support a pressure difference. The strength of this vortex depends on blade number and blade solidity and it is through models of this 'tip effect' that the effect of blade number on rotor performance is expressed in BEM theory. Various tip effect models have been developed (see Section 1.13.2). The most commonly used model in BEM theory is due to Prandtl [32] and that model is adopted in the following analyses.

Adopting the Prandtl tip factor, $F = \frac{2}{\pi}\cos^{-1}(e^{-\pi s/d})$ where $d = \frac{2\pi R(1-a)}{B\lambda}$ and $s = (1-x)R$:

$$F = \frac{2}{\pi}\cos^{-1}\left[\exp\left\{-\frac{(1-x)B\lambda}{2(1-a)}\right\}\right] \tag{1.50}$$

With the assumptions that $a = 1/3$ in optimum operation, that a is constant over the span and knowing the value of lift coefficient at maximum lift to drag ratio for the aerofoil section selected at each radial station, Equation 1.46 then defines the chord distribution of an optimum rotor as a function of radius fraction, x and design tip speed ratio, λ. If the approximations of neglecting a', neglecting the very minor effect of drag and neglecting tip effect are combined with the further approximation of neglecting $(1-a)^2$ in comparison to $\lambda^2 x^2$, Equation 1.46 then reduces to:

$$\Lambda(\lambda, x) = \frac{8\pi a\,(1-a)}{B\lambda^2 x} = \frac{16\pi}{9B\lambda^2 x} \tag{1.51}$$

Equations similar to Equation 1.51 have appeared in various forms, in Gasch and Twele [37], Burton and Sharpe [38], and are easily understood intuitively. Lift per blade element is proportional to dynamic pressure and chord width. Dynamic pressure on a blade element is proportional to the square of the inflow velocity which is predominantly the in-plane velocity when $\lambda > 6$. Thus to maintain total rotor lift at the appropriate fixed optimum value, $\Lambda(\lambda, \mathrm{x})$ must approximately vary inversely as $B\lambda^2 x$.

Equation 1.46 (or its simplified forms such as Equation 1.51) allows the optimum chord distribution of a blade to be developed given a selection of aerofoil types that will then define at each radial station, x, the maximum lift to drag ratio, k, the associated design lift coefficient, C_L and the corresponding angle of incidence, α_0. An optimum blade twist

distribution is then determined referring to Equation 1.39 and setting $a = 1/3$ as:

$$\theta(x) = \tan^{-1}\left\{\frac{2}{3\lambda x\,(1+a')}\right\} - \alpha_0(x) \cong \frac{2}{3\lambda x} - \alpha_0(x) \tag{1.52}$$

As far as optimal blade shape is concerned, the simplified Equation 1.51 predicts the chord distribution very well over the extent of span that most matters. It would be usual in real designs to round the tip in a way that may be guided by practical experience or CFD analyses and, for practical reasons associated with manufacture and/or transportation, to limit the chord to much less than ideal values inboard of say 20–25% span. With the chord being so limited, and the sections normally transitioning to a cylindrical blade root end, there is then no point to continue the twist distribution near the blade root to the very high angles that would be predicted by Equation 1.52. In that case, the approximate form of Equation 1.52 is a good estimate over the aerodynamically active part of the rotor.

As was discussed, the optimum lift force on each blade element specifies the product, cC_L, in Equation 1.37. This means that the chord width can be optimised structurally if aerofoils are available or can be designed with suitable values of design lift coefficient C_L. Thus, as is discussed further in Chapter 2, for the same blade design tip speed ratio, aerofoils with high or low design C_L can enable slender or wide optimum blades.

There is however constraint on having rapid changes in the spanwise variation of C_L. A basic principle is that it is generally undesirable to have rapid changes in section lift (specifically lift and not lift coefficient) along the span of the blade. The trailing vortices which generate induced drag (or the induction factor for a rotor) are proportional to the spanwise gradient of lift (actually circulation but effectively the same). A sudden change in blade chord is undesirable structurally and aerodynamically; this implies that C_L should not change abruptly since the relative inflow velocity varies only gradually with radial position. It is therefore usually assumed that a constant[6] C_L is desirable over most of span with a smooth reduction to zero at the tip.

Having characterised the optimum lift distribution as in Equation 1.46, expressions generally useful for parametric studies are now derived for the power coefficient, thrust coefficient and out-of-plane bending moment coefficient (to be defined). The torque coefficient, $C_q = \frac{Q}{0.5\rho V^2 \pi R^3}$, where Q is the rotor torque, is sometimes useful in evaluating the self-starting capability of wind turbines and is trivially related to the power coefficient as $C_q = \frac{C_p}{\lambda}$.

Examination of the simple actuator disc Equations 1.9 and 1.16 and also results from BEM calculations will show that the thrust coefficient C_t is rising quite rapidly with respect to both axial induction and tip speed ratio around the point of maximum C_p. Thus a practical trade-off in the the design of optimised rotors is to reduce design tip speed ratio and operate a little below the strictly maximum C_p thereby gaining a useful reduction in loads.

[6] The optimum spanwise distribution of circulation or lift on a fixed wing is a smooth elliptic variation (which was provided uniquely at all angles of attack by the Spitfire wing), but there may not be any simple theory to define the optimum shape for a rotor.

1.11.1 The Power Coefficient, Cp

Returning to Equation 1.38:

$$dQ = \frac{1}{2}\rho W^2 Bcr\left(C_L \sin\varphi - C_D \cos\varphi\right) dr \tag{1.53}$$

Hence elemental power is:

$$dP = \frac{1}{2}\rho W^2 Bc\ r\left(C_L \sin\varphi - C_D \cos\varphi\right)\omega dr \tag{1.54}$$

$$= \frac{1}{2}\rho\left(\frac{W}{V}\right)^2 R^2 V^3 \Lambda\left(\lambda, x\right) B\left(\sin\varphi - \frac{\cos\varphi}{k}\right)\lambda x\, dx. \tag{1.55}$$

and the rotor power coefficient is:

$$C_p = \frac{B}{\pi}\int_0^1 \Lambda\left(\lambda, x\right)\left(\frac{W}{V}\right)^2\left(\sin\varphi - \frac{\cos\varphi}{k}\right)\lambda x\, dx. \tag{1.56}$$

Substituting for W/V, $\sin\varphi$ and $\cos\varphi$ from Figure 1.8 and for $\Lambda\left(\lambda, x\right)$ from Equation 1.46:

$$C_p = \frac{B}{\pi}\int_0^1 \frac{8\pi a\left(1-a\right).F}{B\lambda\left(1+a'\right)}\frac{\lambda\left\{\left(1-a\right) - \dfrac{\lambda x\left(1+a'\right)}{k}\right\}xdx}{\left\{1 + \dfrac{\left(1-a\right)}{k\lambda x\left(1+a'\right)}\right\}}. \tag{1.57}$$

Considering a rotor without tip effect, neglecting a' and neglecting also $\frac{(1-a)}{k\lambda x\left(1+a'\right)}$:

$$C_p = 8a\left(1-a\right)\int_0^1\left\{\left(1-a\right) - \frac{lx}{k}\right\}xdx \tag{1.58}$$

and hence:

$$C_p = 4a\left(1-a\right)^2\left[1 - \frac{2\lambda}{3k\left(1-a\right)}\right] \tag{1.59}$$

Equation 1.59, as it must, tends to the actuator disc result of Betz as $k \to \infty$. With k finite, it is similar to a limiting case derived by De Vries [39] which arose from a quite different beginning in the context of BEM theory for vertical axis wind turbines. De Vries' equation is:

$$C_p = 4a\left(1-a\right)^2 - \frac{BcC_D\lambda^3}{2R} \tag{1.60}$$

Noting that $\frac{BcC_D\lambda^3}{2R} = B\left(\frac{cC_L}{R}\right)\frac{\lambda^3}{2k}$ and also considering Equation 1.51, the Equations 1.59 and 1.60 have a similar form.

Returning to Equation 1.57, the general expression for C_p can be expressed as:

$$C_p(\lambda) = \int_0^1 \frac{8a\,(1-a)\,F\left[k\,(1-a) - \lambda x\left(1+a'\right)\right]\lambda x^2}{[\mathrm{k}\lambda \mathrm{x}\,(1+\mathrm{a}') + (1-a))]}\,dx \tag{1.61}$$

Equation 1.61 is a rigorous BEM relationship defining C_p first published, Jamieson [40], without derivation. As was mentioned in connection with Equation 1.47, the lift to drag ratio, k, is a function of angle of attack $\alpha\,(\mathrm{x}) = \varphi\,(\mathrm{x}) - \theta\,(x) - \psi$ and the flow angle $\varphi\,(x)$ is therefore implicitly present in Equation 1.61.

However, in the optimum rotor state, for typical design tip speed ratios above say about 6 and with typical aerofoil selections for large HAWTs, it is a very good approximation to assume that all the blade elements operate at their maximum lift to drag ratio, $k \equiv k\,(x)$ and, using Equation 1.47 or 1.48 to determine a', Equation 1.61 can then be directly integrated. Hence maximum C_p may be expressed as a function of tip speed ratio and lift to drag ratio as in Figure 1.9. Although for convenience in the calculations presented in Figure 1.9, the lift to drag ratio is treated as constant over the blade span, there is no requirement for this to be the case. If k is defined as a function of x, Equation 1.61 can be used for a rotor with differing aerofoil characteristics over the span, as is usually the case on account of thickness to chord ratio decreasing from root to tip.

A chart such as Figure 1.9 has been published previously [41], but the results were determined by numerical solution of the BEM equations and not from an explicit formula. After such an exercise, Wilson *et al*. [33] fitted data with the formula (Equation 1.62) which was claimed valid for $4 \leq \lambda \leq 25$, and $k = Cl/Cd \geq 25$ but restricted to three blades maximum.

$$C_{p.\max} = \left(\frac{16}{27}\right)\lambda\left[\lambda + \frac{1.32 + \left(\dfrac{\lambda - 8}{20}\right)^2}{B^{2/3}}\right]^{-1} - \frac{(0.57)\,\lambda^2}{\dfrac{C_l}{C_d}\left(\lambda + \dfrac{1}{2B}\right)} \tag{1.62}$$

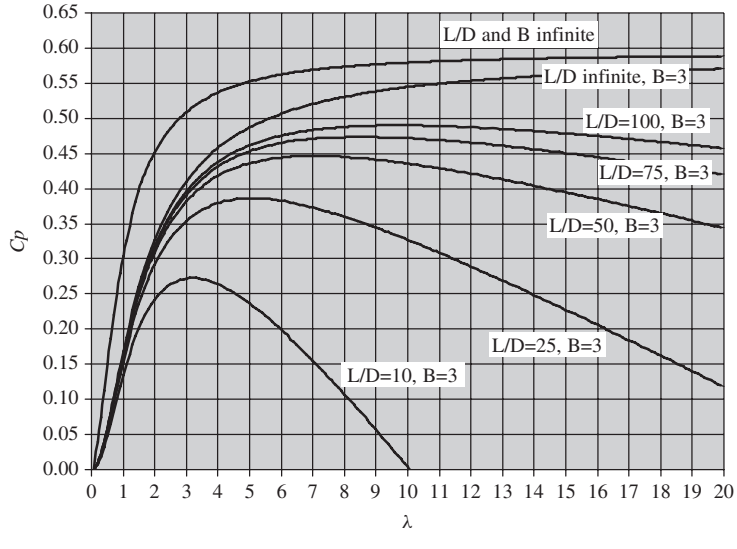

Figure 1.9 C_p max v tip speed ratio for various lift to drag ratios

Some general similarity between this empirical relation Equation 1.62 and Equation 1.59 may be noted with the additional complexity in Equation 1.62 taking account of tip effects over the range of applicability.

It will be evident (Figure 1.9) that for any given blade number, B and maximum lift to drag ratio, k, there is a unique optimum value of tip speed ratio, λ to maximise C_p. Figure 1.10 shows C_p max as a function of design tip speed ratio for a range of lift to drag ratios and blade numbers. As is confirmed in Figure 1.10 (and also Figure 1.9), a typical state of the art blade for a large wind turbine designed for a tip speed ratio of around 9 and with average equivalent maximum lift to drag ratio around 100 will achieve C_p max of approximately 0.5. While Figure 1.9 shows appropriate trends, without a full solution of the BEM equations, Equation 1.61 using the assumption of k constant at a maximum value for the chosen aerofoils will only predict C_p curves accurately in the region of C_p max.

Figure 1.10 clarifies an important point that to maximise the benefit from aerofoils that may achieve higher lift to drag ratios, it is important to design for new (higher) optimum tip speed ratios. Figure 1.10 also provides a clear and immediate indication of how optimum one, two, three or multi bladed rotors will compare in power performance for any given choice of aerofoils whilst Figure 1.9 clarifies the penalties that may apply in operating at non-optimum combinations of lift to drag ratio and design tip speed ratio.

Equation 1.61 shows that C_p is a complex function of the axial induction, a. The result that $a = 1/3$ results in maximum rotor C_p was based on simple actuator disc theory (Equation 1.9) and this clearly cannot be exactly true for Equation 1.61. It may also be noted from that from Equation 1.53, it is only plausible and not rigorous that maximising $k = C_L/C_d$ will

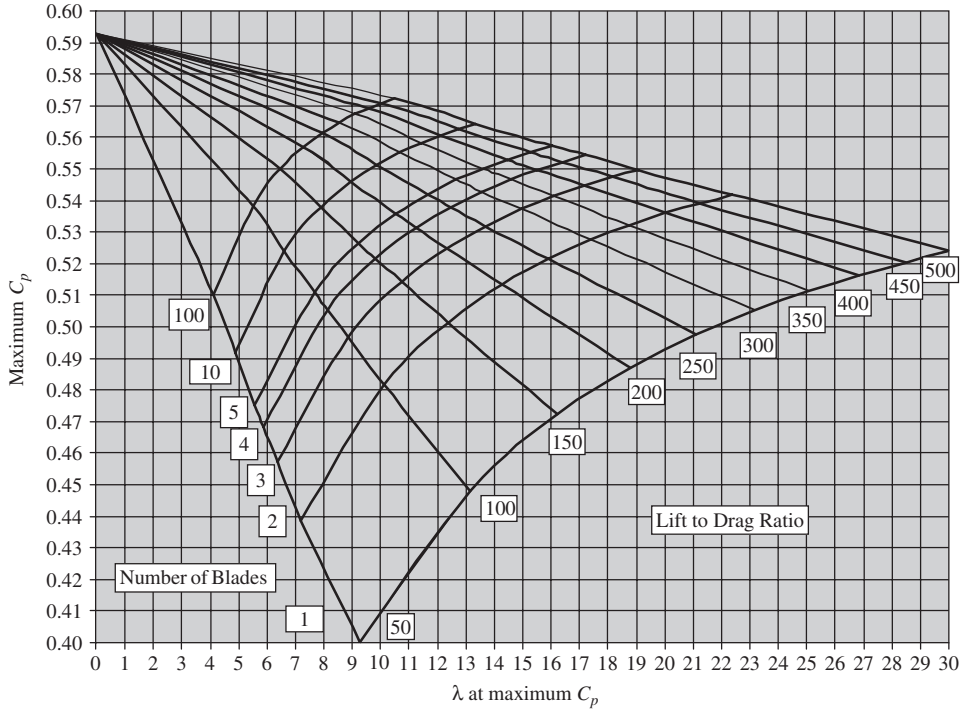

Figure 1.10 Influence of blade number and lift to drag ratio on maximum C_p

maximise the torque on each blade element as the elemental torque clearly also depends on flow angle, φ and how it may vary with k in the course of a full solution of the BEM equations. Considering Equation 1.55, a power coefficient can be defined local to each blade element as:

$$C_p(r, a, k) = \frac{dP(r, a, k)}{0.5\rho V^3 (2\pi r dr)} \tag{1.63}$$

A strict optimisation according to the BEM theory presented will maximise $C_p(r, a, k)$ separately on each blade element. This results in a varying spanwise and k near to maximum but not absolutely maximum on each aerofoil section. For typical large electricity producing wind turbines with design $\lambda \geq 6$ and $k \geq 100$, in an ideal optimum blade design, a is little different from 1/3 over most of the span and k is very close to the maximum for each aerofoil section. These effects are rather more significant however, for a rotor based on aerofoils with low lift to drag ratio, for example sailcloth blades or plate blades. The non-uniformity of an optimum distribution of axial induction is not of practical importance for optimum rotor design because of the limitations of BEM theory in its present form. Other issues appear in more accurate optimisation methods (see Section 1.13.3). However, based on the BEM equation system in a standard form, the non-uniformity of axial induction (i.e. not exactly constant at a value of 1/3 over the whole span) of an optimum rotor is a consistent outcome and is mentioned for that reason.

1.11.2 Thrust Coefficient

In a similar way to the derivation of maximum C_p from Equation 1.35 to Equation 1.61, the associated thrust coefficient can be determined as;

$$C_T = \int_0^1 8a(1-a) F x dx \tag{1.64}$$

In the limit of no tip loss ($F = 1$), the familiar actuator disc formula, $C_T = 4a(1-a)$, is recovered with $C_T = 8/9$ for an optimum rotor. Equation 1.64 has a much simpler form than Equation 1.61. The thrust coefficient is a *system* property dependent on rotor loading but independent of the efficiency of the rotor in power conversion. It is therefore unaffected by lift to drag ratio or the tangential induction factor and dependent only on the state of rotor loading characterised by the axial induction over the rotor plane which is naturally influenced by the tip effect.

1.11.3 Out-of-Plane Bending Moment Coefficient

The steady state out-of-plane bending moment of an optimised blade in operation at its design tip speed ratio below rated wind speed and the introduction of pitch action may be derived from any standard BEM code and has a characteristic shape as in Figure 1.11. For typical large scale electricity generating wind turbines, that is well optimised rotor designs with design tip speed ratios above 6, the shape is largely independent of design specifics and can usually be very well approximated by a cubic curve. Such representations have been convenient in studies developing blade designs embodying passive aeroelastic control

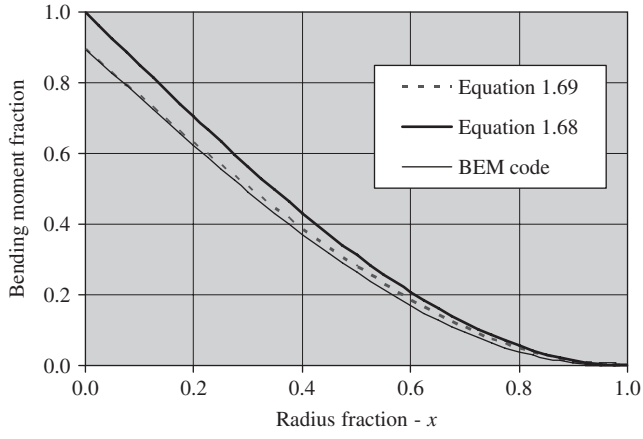

Figure 1.11 Out-of-plane bending moment shape functions

(e.g. with flap-twist coupling as in Maheri [42]) where a simplified representation of blade loading is useful. BEM theory provides a simple derivation of the result as follows.

Defining a dimensionless bending moment coefficient at arbitrary radial distance, r, as $C_M(r) = \frac{M(r)}{(0.5\rho V^2 \pi R^3)}$ and following similar methods of analysis as for C_p in Equations 1.35–1.61 lead to:

$$C_M(r) = \frac{8a(1-a)}{B} \int_x^1 \frac{F(y)}{\left\{(1+a')\lambda y + \frac{(1-a)}{k}\right\}} \cdot \left\{\lambda y + \frac{(1-a)}{k}\right\} (y-x)\, y dy \tag{1.65}$$

Neglecting a' in comparison to unity gives:

$$C_M(x) = \frac{8a(1-a)}{B} \int_x^1 F(y)(y-x) y.dy \tag{1.66}$$

Considering the case with no tip effect where $F(y) = 1$:

$$C_M(x) = 4a(1-a)\left\{\frac{1}{3B}\left(2 - 3x + x^3\right)\right\} \tag{1.67}$$

And for an optimum rotor, taking $a = 1/3$:

$$C_M(x) = \frac{16}{27B}\left\{\frac{(x-1)^2(x+2)}{2}\right\} \tag{1.68}$$

For a typical conventional three bladed wind turbine, Equation 1.68 has the appropriate cubic shape but, because the bending moment is most heavily weighted by the loading which is farthest outboard, the tip effect is very significant in relief of blade root bending moment.

Wilson (see Spera [41], Chapter 5, p. 261) and Milborrow [43] (a paper offering a variety of useful simplified parametric equations for blade loads) have previously derived an equation similar to 1.68. Wilson [44] noted that this relationship predicted values significantly greater than measured blade bending moment data from the Mod-2 HAWT. He further observed that the Mod-2 blade design was far from an optimised configuration and described Equation 1.68 as 'an upper bound' which it is for an optimum rotor without tip loss. However, noting the more general form of Equation 1.67, the bending moment coefficient is unsurprisingly related to the thrust coefficient which is not maximised at $a = 1/3$ even in the ideal inviscid model without considering higher loadings that may result in the turbulent wake state. Thus sub-optimal rotors may have bending moment characteristics that exceed (or are within) the predictions of Equation 1.68.

A direct application of Equation 1.68 will overestimate the moment at shaft centreline of an optimum three bladed rotor with a design tip speed ratio of $\lambda = 7$ by about 13%. Equation 1.66 is therefore not immediately appropriate for use in parametric studies without some adjustment to account for the tip effect.

Equation 1.69 is a useful approximation to Equation 1.62 which can represent the blade root moment quite accurately when (as is the case for mainstream electricity generating wind turbines) the product of blade number and design tip speed ratio, $B\lambda > 10$.

$$C_M(x) = \frac{16}{27B} G(B\lambda)\, f(x) \tag{1.69}$$

Where:

$$G(B\lambda) = 5.5744 \times 10^{-7} B^3\lambda^3 - 8.2871 \times 10^{-5} B^2\lambda^2 + 4.4085 \times 10^{-3} B\lambda + 2.3245 \times 10^{-1} \tag{1.70}$$

and

$$f(x) = \frac{(x-1)^2 (x+2)}{2} \tag{1.71}$$

In retaining the simple cubic function, $f(x)$, and providing an accurate match to the blade root bending moment, Equation 1.69 is somewhat conservative in blade out-of-plane bending moment estimates on the outboard blade. Accuracy in estimation of blade root bending moment is probably of greatest interest in parametric studies and, for a three bladed wind turbine with $\lambda = 7$, Equation 1.69 gives $C_M(0)$ as 0.8809 whilst integration of Equation 1.65 using the Prandtl tip loss factor gives a corresponding value of 0.8827.

1.12 Generalised BEM

The generalised actuator disc results of Sections 1.5 and 1.6 can be used to derive a generalised BEM that will assist in the optimisation of rotors in ducts or diffusers. In order to revise the BEM equations for generalised flow conditions, consider first the elemental thrust and axial momentum balance:

The mass flow rate through the rotor plane is, $\dot{m} = \rho (2\pi r \mathrm{d}r) \{V(1-a)\mathrm{F}\}$.

The total change in flow velocity between far upstream and far wake (see Table 1.1) is:

$$dV = V\left\{1 - \left(\frac{1 - 2a + a_0}{1 - a_0}\right)\right\} = \frac{2V(a - a_0)}{(1 - a_0)} \tag{1.72}$$

However, considering the thrust force on the rotor alone (see Equation 1.32):

$$dT = 4\pi\rho r V^2 \frac{(a - a_0)(1 - a)}{(1 - a_0)^2} F dr \tag{1.73}$$

Equation 1.38 is unchanged and hence:

$$dQ = 4\pi\rho r^3 V a' \omega (1 - a) F dr \tag{1.74}$$

Equations 1.37, 1.38 and 1.41 are also unchanged. The tangential induction factor, a' may be approximated by neglecting drag and generalised as:

$$a'\left(1 + a'\right) = \frac{(1 - a)(a - a_0)}{(1 - a_0)\lambda^2 x^2} = \frac{C_t (1 - a_0)}{4\lambda^2 x^2} \tag{1.75}$$

The further development of the generalised BEM model is simplest if a_0 is assumed to be a suitably averaged constant value over the rotor disc and that is tacitly assumed in the following analyses. However there is no requirement for this and a variation of $a_0 \equiv a_0(r, \theta)$ may be defined over the rotor disc.

An analogue to Equation 1.46 may be developed or the equation system in the generalised flow case may be solved by iterative numerical methods in the same way as in standard BEM.

The associated non-dimensional lift distribution is:

$$\Lambda(\lambda, x) = \frac{2\pi C_t}{B\lambda (1 + a')\sqrt{(1 - a)^2 + \lambda^2 x^2 (1 + a')^2}} \frac{F}{\left[1 + \frac{(1 - a)}{k\lambda x (1 + a')}\right]} \tag{1.76}$$

For an optimum rotor, $a = a_{.m} = \frac{1+2a_0}{3}$ and $C_t = \frac{8}{9}$.

If the maximum lift to drag ratio of a chosen aerofoil section occurs at an angle of incidence $\alpha = \alpha_{0,}$ then the optimum twist distribution is given as:

$$\psi(x) = \tan^{-1}\left\{\frac{2(1 - a_0)}{3\lambda x (1 + a')}\right\} - \alpha_0 \tag{1.77}$$

The optimum twist distribution will evidently vary with a_0 and hence may vary significantly according to the nature of the system affecting the rotor plane induction. Suppose there is substantial flow augmentation at the rotor plane. As $C_t = 8/9$ universally, the rotor is optimally loaded at exactly the same value of thrust coefficient and thrust as in open flow with no augmentation system present. This implies that the blade elements must be pitched much further into the flow direction so that a reduction in the lift component producing thrust exactly compensates for the potential increase in thrust due to the augmented local flow velocity. However in this situation there is then a much larger lift contribution to rotor torque than in open flow. This corresponds to the increased power performance coefficient which may exceed the Betz limit in proportion to the flow augmentation achieved.

The usual actuator disc theory whether standard or generalised considers only inviscid flow. In order to be more realistic and useful for design calculations, empirical modelling is introduced to represent the thrust coefficient in the turbulent wake state. Experimental validation for systems with concentrators is not yet available, and so the results derived represent no more than a consistent extension from the standard open flow model to the generalised actuator disc theory.

If a is the induction at the rotor plane in open flow, then the transformation, $a \rightarrow \frac{a-a_0}{1-a_0}$, determines the value of axial induction at a plane (not the rotor plane) in constrained flow where the induction is half of that in the far wake. However, as is explained in Jamieson [29], the value of thrust coefficient, C_t, is independent of location in the system. Therefore this transformation may be employed to determine an expression for thrust coefficient that is applicable at the rotor plane.

In open flow, various formulations are employed to modify the thrust coefficient equation of the inviscid flow actuator disc as the rotor approaches the turbulent wake state. GL Garrad Hassan's commercial BEM software package, *Bladed*, defines thrust coefficient, C_t, as:

$$C_t = 4a\,(1-a) \quad for\ 0 \le a \le 0.3539 \tag{1.78}$$

$$C_t = 0.6 + 0.61a + 0.79a^2 \quad for\ 0.3539 < a \le 1 \tag{1.79}$$

In generalised flow states, applying again the transformation of Equation 1.69 results in the equations:

$$C_t = \frac{4\,(a-a_0)\,(1-a)}{(1-a_0)^2} \quad for\ 0 \le a \le a_0 + 0.3539\,(1-a_0) \tag{1.80}$$

$$C_t = 0.6 + 0.61\left\{\frac{a-a_0}{1-a_0}\right\} + 0.79\left\{\frac{a-a_0}{1-a_0}\right\}^2 \quad \text{for } a_0 + 0.3539\,(1-a_0) < a \le 1 \tag{1.81}$$

Equation 1.78 does not accurately accord with BEM theory as reflected in Equation 1.64 where the tip effect modifies the thrust coefficient. Thus the method of application is to factor the C_t in the BEM solutions as a ratio of Equations 1.79 or 1.81 to the corresponding actuator disc Equations 1.78 and 1.80.

In open (unconstrained) flow the thrust coefficient is essentially unique and optimum at 8/9 at least in the ideal inviscid flow case. However, as is elaborated in Jamieson [29], in constrained flow, the thrust coefficient is a system property. Irrespective of rotor efficiency, C_t in an ideal system is optimally 8/9 and maximises C_p at that value. If the system is not *ideal* in the optimal rotor loading state (which for a diffuser would mean that the diffuser is not fully optimised for the flow field that will develop in operation at a rotor thrust coefficient of 8/9), then the C_t that maximises C_p will be less than 8/9 and the associated maximum C_p will be less than it would be in an ideal system. On the other hand any external mass flow (i.e. flow not passing through the rotor) that influences the overall energy exchange, for example by assisting wake transport, may increase the optimum C_t at the rotor plane to above 8/9. Results of Phillips *et al*. [45] suggest that in a well designed diffuser, an optimum C_t of around unity may be achieved.

Great care is required in applying generalised BEM to real systems but the new theory offers a rationalised approach and parametric insight for the optimisation of rotor design in flow concentrators that has not been previously available. The general approach as in Jamieson [46] will be to replace a_0 with $\eta\,(a)\,a_0$ where $\eta\,(a)$is a system efficiency function to be defined from empirical information, CFD analyses or otherwise. Also the estimation of a_0 is not straightforward as is also discussed in Jamieson [46].

Nevertheless the introduction of the variable a_0 characterising flow augmentation in conjunction with the indicated generalisation of the thrust coefficient indicates an extension of BEM theory which is simple to implement and can address the design of rotors in flow concentrators.

It is also important to be aware of systems where ducted rotors may be used and the generalised BEM theory developed here will not be applicable as in the case of a tidal

turbine where distances from the free water surface and sea bed are not large compared to the rotor dimensions. In such a case Bernoulli's equation with only pressure and velocity terms (the usual basis of wind turbine actuator disc models) is insufficient and an adequate model [47] must account for buoyancy terms as the pressure drop behind the turbine will induce a local drop in sea surface level.

The analytical relationships developed in the foregoing discussion of BEM theory can be bypassed in the use of the usual numerical methods for BEM solutions. However identification of explicit formulae is considered to be of great value in design development, facilitating preliminary parametric studies that provide insight into how some of the key variables in rotor design may influence performance. This will be revisited later in the context of specific case studies.

1.13 Limitations of Actuator Disc and BEM Theory

1.13.1 Actuator Disc Limitations

In spite of the great practical value of his actuator disc concept, Froude was aware of unresolved issues specially in regard to what happens at the edge of the disc. Van Kuik [23] suggests that both experimental evidence and limitations in modelling effects at the edge of the actuator disc (in open flow) indicate that higher velocities than predicted by Froude's theorem (that the rotor plane velocity is the average of upstream and far wake velocities) occur at the rotor plane. This, he argues, is equivalent to having edge forces which induce extra flow through the disc (implying a slight flow augmentation with $a_0 < 0$, in terms of the generalised actuator disc model of Section 1.5). This is considered to apply even in the ideal inviscid case and is not due to wake entrainment by external flows which may also enhance the performance of a rotor in real wind conditions.

1.13.2 Wake Rotation and Tip Effect

The so-called tip effect essentially differentiates rotors of similar solidity, aerofoil selection and design speed in terms of blade number. In the limit of an infinite number of infinitely slender blades travelling at infinite rotation speed, all the power is produced without a torque reaction or wake rotation.

Assuming a uniform wind field upstream of the rotor with no intrinsic rotating structures or initial angular momentum, the creation of angular momentum in the wake of the rotor is predicted for all real rotors with a finite number of blades and finite speed which implies in turn a non-zero torque reaction.

This is not in question but De Vries [39] and later Sharpe [48] have made the case for the view that wake angular momentum is associated with a reduction in wake core static pressure that arises conservatively from the blade circulation. This contradicts the conventional BEM modelling of Wilson, Lissaman and Walker as presented in this text. Recent CFD modelling, Madsen *et al.* [49], has supported the De Vries interpretation. This is significant for the physical interpretations underlying BEM theory and for the accuracy of detailed design calculations on rotor aerodynamics. It little affects the top level parametric analyses and formulae developed in Section 1.10 as applied to rotors with design tip speed ratios above about 6. It will matter especially in detailed aerodynamic design of rotors around the hub and tip areas especially and have substantial implications for rotors with very low design tip speed ratio.

There are a number of tip effect models (see Shen *et al*. [50] for example). The Prandtl model has been employed as the simplest available, purely for convenience, having in mind that differentiating these models or getting into accurate correspondence with real tip flows moves into territory where the simple BEM theory is generally inadequate. It should also be noted that there are also a number of different approaches in the application of the tip factors that differ in detail from Equations 1.35 and 1.36 including an elegant model due to Anderson [51] which accounts for cyclic variation in the induction factors.

1.13.3 Optimum Rotor Theory

It has been mentioned that the optimum rotors produced by BEM theory differ a little from those developed with the ideal actuator disc assumption that the axial induction is 1/3 everywhere over the rotor span. These differences are considered unimportant because BEM theory is not accurate enough for them to be really meaningful. Recent work of Madsen [52] on optimum rotor design following from the previous work [49] also suggests that classical BEM solutions for optimum rotors will not be very accurately optimal. This is important both at a fundamental level and for practical detailed design of optimum rotors but does not particularly undermine the value of equations such as 1.51 for guiding parametric design investigations.

1.13.4 Skewed Flow

A major weakness of BEM theory is in modelling wind turbines in yawed flow. When the flow is oblique to the rotor plane, there are cyclic variations in angle of attack which can be important especially when flow angles approach stall. The strip theory assumption that the rotor can be analysed as annular elements that are independent of each other is less justifiable. Dynamic stall behaviour and stall hysteresis can have greater effect on rotor performance. Also in yawed flow there are additional issues about the wake. Does it remain symmetric about the rotor axis or is it skewed in the wind direction? Experimental evidence and CFD analyses indicate the latter and skewed wake correction as for example based on Glauert [53] have been applied in using BEM to model yawed flow. BEM theory can adopt simplifying assumptions (such as taking account of the angle of the wind vector in the inflow calculations), can incorporate dynamic stall models and yield useful results. However, in yawed flow, there is much less certainty in basic calculations (even such as the determination of average rotor power) than in cases where the wind direction is normal to the rotor plane. In general more sophisticated aerodynamic modelling using vortex wake models [9, 54], or CFD is desirable.

1.13.5 Summary

The limitations of BEM have been highlighted. CFD and vortex theory based analyses may be more accurate in many circumstances. Nevertheless, although huge advances have been made in recent years and progress will continue, current CFD techniques do not yet solve the Navier Stokes equations with the same objectivity as mother nature. Turbulence, transition and boundary layer modelling remain problematic. Some vortex wake models assume Froude's theorem and some CFD analyses are calibrated to reproduce actuator disc

results. It is through a mixture of techniques and convergence of insights coupled with experimental feedback that progress is made.

References

[1] Breton, S.-P. (2008) Study of the stall delay phenomenon and of wind turbine blade dynamics using numerical approaches and NREL's wind tunnel tests. Doctoral theses at NTNU, p. 171. ISBN: 978-82-471-1019-5.

[2] Chaviaropoulos, P.K. and Hansen, M.O.L. (2000) Investigating three-dimensional and rotational effects on wind turbine blades by means of a quasi-3D Navier Stokes solver. *Journal of Fluids Engineering*, **122**, 330–336.

[3] Raj, N.V. (2000) An improved semi-empirical model for 3-D post stall effects in horizontal axis wind turbines. Master of Science thesis in Aeronautical and Astronautical Engineering, University of Illinois at Urhana-Champaign, Urhana, IL.

[4] Himmelskamp, H. (1947) Profile Investigations on a Rotating Airscrew. MAP Volkenrode Report and Translation No. 832.

[5] Snel, H., Houwink, R., van Bussel, G.J.W. and Bruining A. (1993) Sectional prediction of 3D effects for stalled flow on rotating Blades and comparison with measurements. 1993 European Community Wind Energy Conference Proceedings, Lubeck-Travemunde, Germany, pp. 395–399.

[6] Rasmussen, F., Hansen, M.H., Thomsen, K. *et al*. (2003) Present status of aeroelasticity of wind turbines. *Wind Energy*, **6**, 213–228. doi: 10.1002/we.98.

[7] Snel, H. (2003) Review of aerodynamics for wind turbines. *Wind Energy*, **6**, 203–211. doi: 10.1002/we.97.

[8] Ostowari, C. and Naik, D. (1985) Post stall studies of untwisted varying aspect ratio blades with NACA 4415 airfoil section part 1. *Wind Engineering*, **9** (3), 149–164.

[9] Simoes, F.J. and Graham, J.M.R. (1990) A free vortex model of the wake of a horizontal axis wind turbine. Proceedings of the 7th BWEA Conference, Norwich, UK, pp. 161–165.

[10] Schreck, S. and Robinson, M. (2002) Rotational augmentation of horizontal axis wind turbine blade aerodynamic response. *Wind Energy*, **5**, 133–150. doi: 10.1002/we.68.

[11] Hoerner, S.F. (1965) *Fluid Dynamic Drag*, Published by the Author.

[12] Krauss, T.A. (inventor) (1986) X-wing aircraft circulation control. US Patent 4,573,871, March 1986.

[13] http://www.rdmag.com/News/2010/01/Energy-More-power-circulation-control-to-alter-wind-turbine-design. Accessed August 2010.

[14] Lewis, R.I. (1991) *Vortex Element Methods for Fluid Dynamic Analysis of Engineering Systems*, Cambridge University Press, Cambridge, p. xix.

[15] Windblat Enercon House Magazine, Issue 3 2008, http://www.enercon.de/www/en/windblatt.nsf/vwAnzeige/4DA5AEEBACEAEDFDC12574A500418221/$FILE/WB-0308-en.pdf.

[16] Di Maria, F., Mariani, F. and Scarpa, P. (1997) Chiralic bladed wind rotor performance. Proceedings of the 2nd European & African Conference on Wind Engineering, Palazzo Ducale, Genova, Italy, June 1997, pp. 663–670.

[17] Holland, R. Jr. (1981) The Holland Roller Windmill. Investigation and Demonstration of Principles. Report No. DOE/R6/10969– T1, DE86 00478, US DOE, June 1981.

[18] http://en.wikipedia.org/wiki/Lift_(force). Accessed August 2010.

[19] Froude, R.E. (1889) On the part played in propulsion by differences in fluid pressure. *Transactions of the Institute of Naval Architects*, **30**, 390.

[20] Bergey, K.H. (1979) The Lanchester-Betz limit. *Journal of Energy*, **3**, 382–384.

[21] van Kuik, G.A.M. (2007) *The Lanchester-Betz-Joukowsky Limit, Wind Energy*, Wiley Interscience.

[22] Okulov, V.L. and van Kuik, G.A.M. *The Betz-Joukowsky Limit: A Contribution to Rotor Aerodynamics by Two Famous Scientific Schools*, Wind Energy, Wiley Interscience. doi: 10.1002/we.464.

[23] van Kuik, G.A.M. (1991) On the limitations of Froude's actuator disc concept. PhD thesis, Technical University of Eindhoven.

[24] Rechenberg, I. (1989) Development and operation of a novel wind turbine with vortex screw concentrator. Second Joint Schlesinger Seminar on Energy and Environment, Berlin, pp. 1–11.

[25] Sforza, P.M. and Stasi, W.J. (1979) Field testing the vortex augmentor concept. Proceedings of Wind Energy Innovative Systems Conference, Colorado.

[26] Oman, R.A., Foreman, K.M. and Gilbert, B.L. (1975) A Progress Report on the diffuser augmented wind turbine. 3rd Biennial Conference and Workshop on Wind Energy Conversion Systems, Washington, DC.

[27] Hansen, M.O.L., Sorensen, N.N. and Flay, R.G.J. (1999) Effect of placing a diffuser around wind turbine. European Wind Energy Conference, pp. 322–324.
[28] Bussel, G.J.W. (2007) The science of making more torque from wind: diffuser experiments and theory revisited. *Journal of Physics: Conference Series, Denmark*, **75**, 1–11.
[29] Jamieson, P. (2008) *Generalised Limits for Energy Extraction in a Linear Constant Velocity Flow Field*, Wind Energy, Wiley Interscience, January 2008.
[30] Lawn, C.J. (2003) Optimisation of the power output from ducted turbines. *Proceedings of the Institution of Mechanical Engineers, Part A: Journal of Power and Energy*, **217**, 107–117.
[31] http://www.flodesignwindturbine.org. Accessed August 2010.
[32] Glauert, H. (1963) Airplane propellers, in *Division L. of Aerodynamic Theory*, vol. **IV** (ed. W.F. Durand), Dover.
[33] Wilson, R.E., Lissaman, P.B.S. and Walker, S.N. (1976) *Applied Aerodynamics of Wind Power Machines*, University of Oregon.
[34] Walker, S.N. (1976) Performance and optimum design analysis/computation for propeller-type wind turbines. PhD thesis, Oregon State University.
[35] Manwell, J.F., McGowan, J.G. and Rogers, A.L. (2008) *Wind Energy Explained*, John Wiley & Sons, Ltd, Chichester, ISBN: 13: 978-0-471-49972-5 (H/B), March 2008.
[36] Betz, A. (1927) NACA Technical Memorandum 474. Die Naturwissenschaften, Vol XV, No 46, November 1927.
[37] Gasch, R. and Twele, J. (2002) *Power Plants: "Fundamentals, Design, Construction and Operation"*, Chapter 8, James & James, October 2002, ISBN: 10: 1902916379, ISBN: 13: 978-1902916378.
[38] Burton, A., Sharpe, D., Jenkins, N. and Bossanyi, E.A. (2004) *Handbook of Wind Energy*, John Wiley & Sons, Ltd, Chichester.
[39] De Vries, O. (1979) *Fluid Dynamic Aspects of Wind Energy Conversion*, AGARDograph, Vol. **243**, NATO, Advisory Group for Aerospace Research and Development, July 1979, ISBN: 92 835 1326-6.
[40] Jamieson, P. (2009) *Lightweight High Speed Rotors for Offshore*, EWEC Offshore, Stockholm.
[41] Spera, D.A. (ed.) (2009) *Wind Turbine Technology: Fundamental Concepts in Wind Turbine Engineering*, 2nd edn, ASME Press.
[42] Maheri, A. (2006) Aero-Structure simulation and aerodynamic design of wind turbines utilising adaptive blades. PhD thesis, Faculty of Computing, Engineering and Mathematical Sciences, UWE, Bristol.
[43] Milborrow, D. (1982) Performance blade loads and size limits for horizontal axis wind turbines. Proceedings of the 4th BWEA Wind Energy Conference, Cranfield BHRA.
[44] Boeing (1982) Mod-2 Wind Turbine System development Final Report, Vol. II, Detailed Report No. NASACR-168007, DOE/NASA/0002-82/2, NASA Lewis Research Centre, Cleveland, Ohio.
[45] Phillips, D.G., Flay, R.G.J. and Nash, T.A. (1999) Aerodynamic analysis and monitoring of the Vortec 7 Diffuser-Augmented wind turbine. *IPENZ Transactions*, **26** (1), 13–19.
[46] Jamieson, P. (2008) Beating Betz–Energy Extraction Limits in a Uniform Flow Field. EWEC 2008, Brussels, March 2008.
[47] Whelan, J., Thomson, M., Graham, J.M.R. and Peiro, J. (2007) Modelling of free surface proximity and wave induced velocities around a horizontal axis tidal stream turbine. Proceedings of the 7th European Wave and Tidal Energy Conference, Porto, Portugal.
[48] Sharpe, D.J. (2004) A general momentum theory applied to an energy-extracting actuator disc. *Wind Energy*, **7**, 177–188. doi: 10.1002/we.118.
[49] Madsen, H.A., Mikkelsen, R., Øye, S. and Bak, Johansen, J. (2007) A detailed investigation of the Blade Element Momentum (BEM) model based on analytical and numerical results and proposal for modifications of the BEM model. The Science of Making Torque from the Wind. *Journal of Physics: Conference Series*, **75**, 012016.
[50] Shen, W.Z., Mikkelsen, R. and Sorensen, J.N. (2005) Tip loss corrections for wind turbine computations. *Wind Energy*, **8**, 457–475. doi: 10.1002/we.153.
[51] Anderson, M.B. (1981) An experimental and theoretical study of horizontal axis wind turbines. PhD thesis, Cambridge University, Cambridge, UK.
[52] Johansen, J., Madsen, H.A.,Gaunaa, M. *et al*. (2009) Design of a wind turbine rotor for maximum aerodynamic efficiency. *Wind Energy*, **12** (3), 261–273. doi: 10.1002/we.292.
[53] Glauert, H. *A General Theory of the Autogyro*. ARCR R&M No.1111, 1926.
[54] Kloosterman, M.H.M. (2009) Development of the Near Wake behind a HAWT including the development of a free wake lifting line code. MSc thesis, TU Delft, 17 June 2009.